

Polyamine-induced modulation of genes involved in ethylene biosynthesis and signalling pathways and nitric oxide production during olive mature fruit abscission
Maria C. Parra-Lobato and Maria C. Gomez-Jimenez.

Supplementary Figures

Supplementary Fig. S1. Phylogenetic analysis of *OeACS* and other ACSs. Gene accession number is shown in parentheses of each gene. The phylogenetic tree was computed using the Clustal-W program (Thompson *et al.*, 1994) employing standard parameters.

Supplementary Fig. S2. Phylogenetic analysis of *OeACO* and other ACOs. Gene accession number is shown in parentheses of each gene. The phylogenetic tree was computed using the Clustal-W program (Thompson *et al.*, 1994) employing standard parameters.

Supplementary Fig. S3. Phylogenetic analysis of *OeERS* and other ERSs. Gene accession number is shown in parentheses of each gene. The phylogenetic tree was computed using the Clustal-W program (Thompson *et al.*, 1994) employing standard parameters.

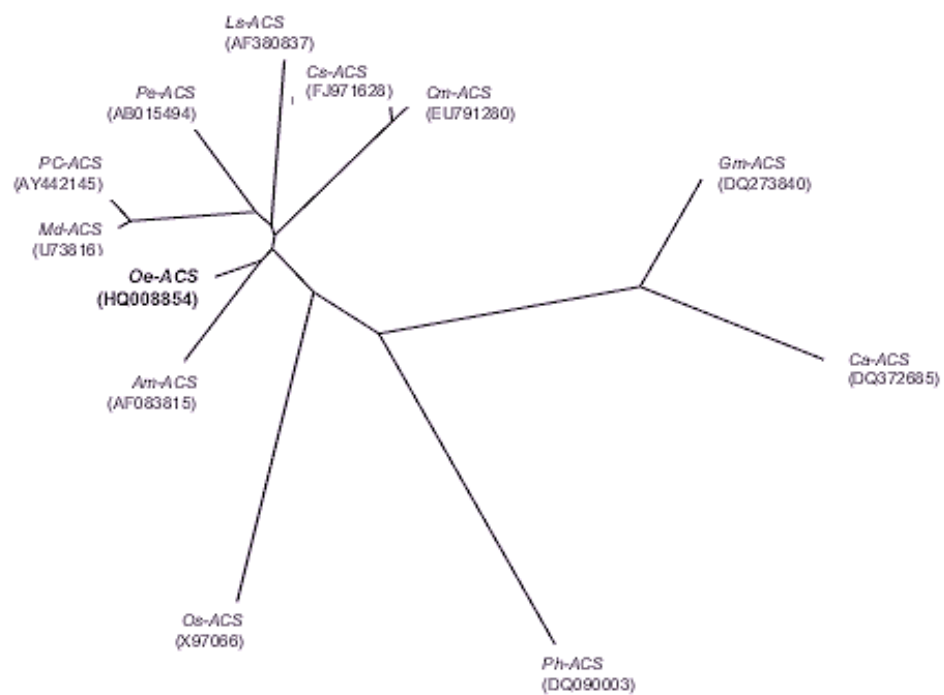
Supplementary Fig. S4. Phylogenetic analysis of *OeCTR* and other CTRs. Gene accession number is shown in parentheses of each gene. The phylogenetic tree was computed using the Clustal-W program (Thompson *et al.*, 1994) employing standard parameters.

Supplementary Fig. S5. Phylogenetic analysis of *OeEIL* and other EILs. Gene accession number is shown in parentheses of each gene. The phylogenetic tree was computed using the Clustal-W program (Thompson *et al.*, 1994) employing standard parameters.

Supplementary Fig. S6. z-Animated 3-D reconstruction of CLSM detection of NO in ARB fruit AZ at 217 DPA with DAF-FM-DA.

Supplementary Fig. S7. z-Animated 3-D reconstruction of CLSM detection of NO in PIC fruit AZ at 217 DPA with DAF-FM-DA.

Fig. S1



0.1

Fig. S2

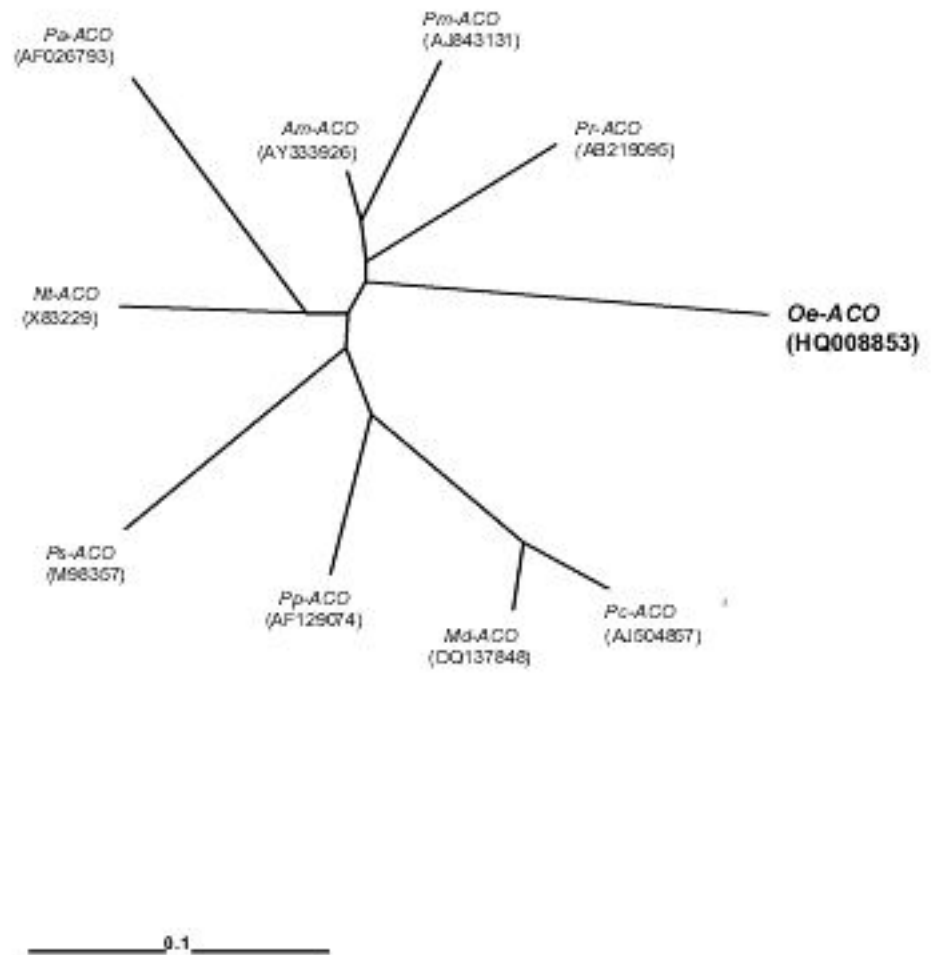
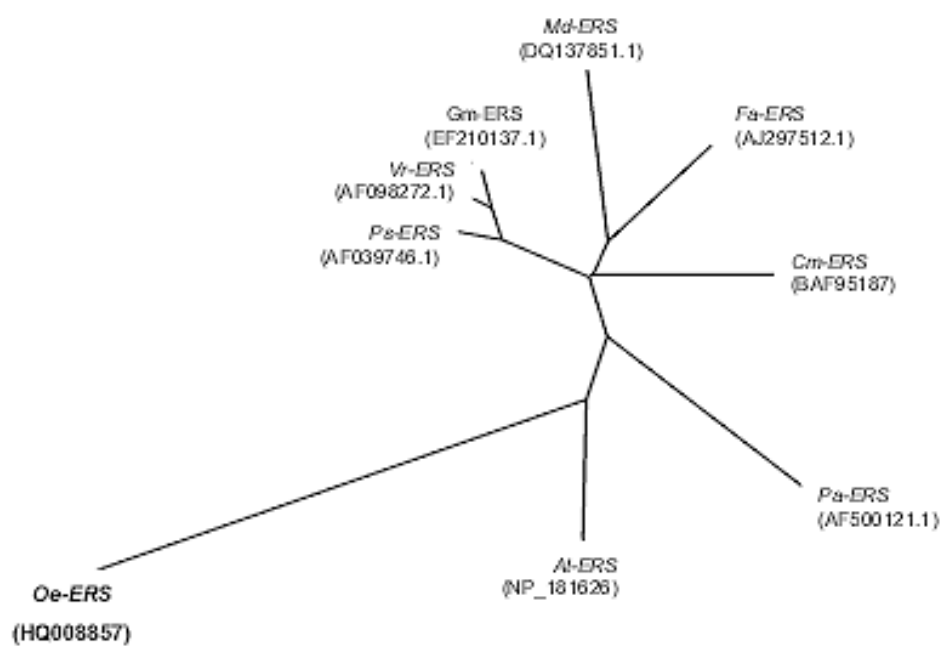
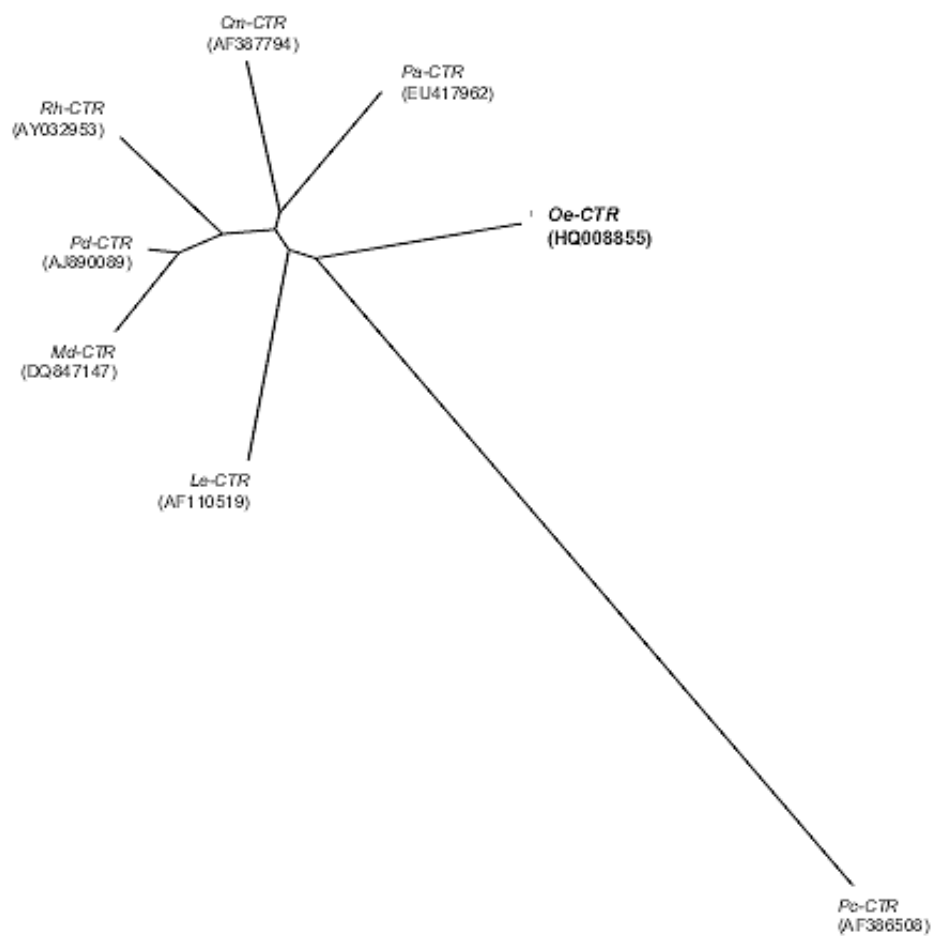


Fig. S3



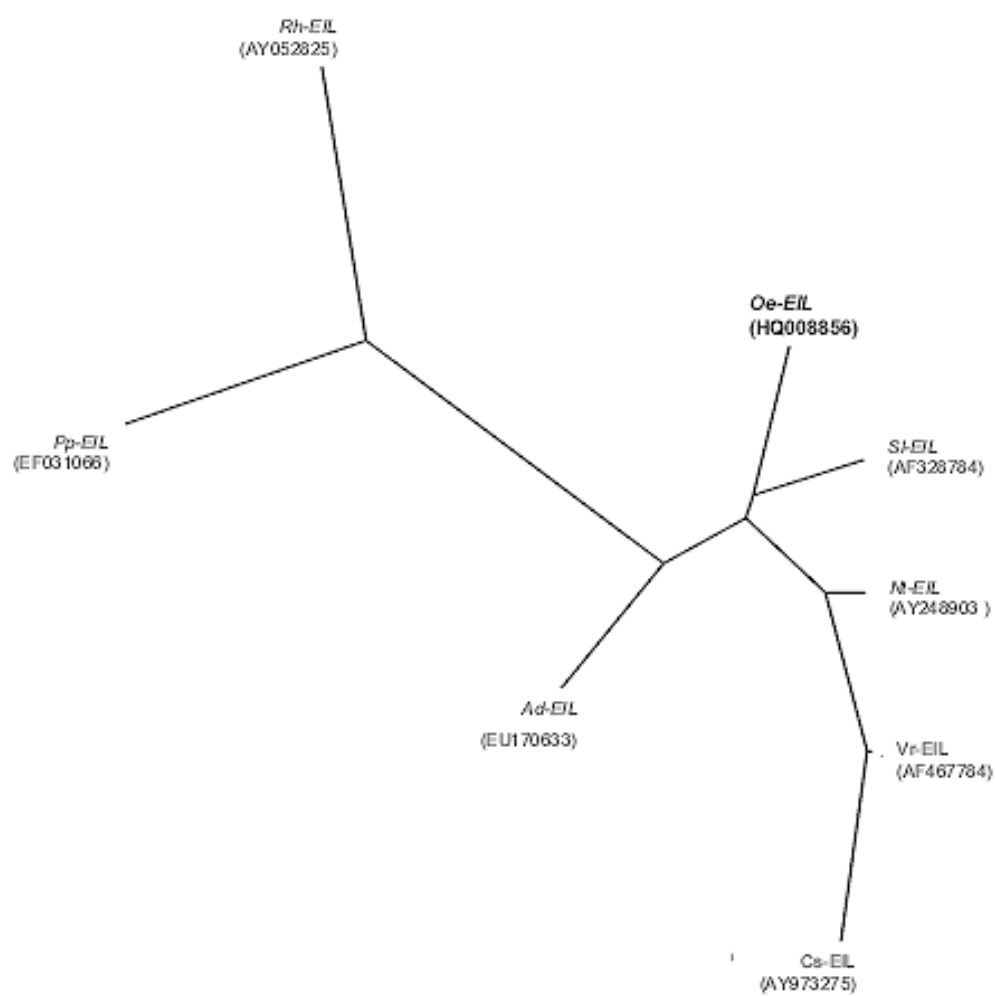
0.1

Fig. S4



0.1

Fig. S5



0.1